PP11: Impact of advanced Higgs boson identification algorithms on the reconstruction efficiency of di-Higgs to 4b final states at the Large Hadron Collider

supervisor: Cigdem Issever
Candidate number:397637
word count:4571

In the study of the *Boosting Higgs Pair Production in the $b\bar{b}b\bar{b}$ Final State with Multivariate Techniques*[1], a constant b-quark tagging efficiency is used for the simulation of the ATLAS detector at LHC. However, a constant b-tagging efficiency is not realistic since the b-tagging efficiency is depending on the transverse momentum of the b-hadrons. Ref.[2]summarizes the Higgs tagging efficiency for advanced taggers. This project aims to answer two question: What is the impact of using the advanced Higgs tagging algorithm with variable tagging efficiency on the signal significance $S/\sqrt{B}$, and what is the maximal $S/\sqrt{B}$? To answer these questions, we will implement the result of the ATLAS pub note[2].

1. INTRODUCTION

The Standard Model (SM) is the currently prevalent and well-understood theory for describing phenomena which occur at the smallest scales. Now that the Higgs boson has been observed by the ATLAS and CMS experiments at the LHC, the next important step would be to measure accurately its properties. Among the measurements which need to be performed, the determination of the Higgs self–coupling is of utmost importance, which it provides crucial information of the electro-weak symmetry breaking mechanism. The only way to determine Higgs self-interaction is by measuring Higgs pair production, which is directly sensitive to the Higgs trilinear coupling constant λ[3](Fig. 1). Also notice that the self-coupling is only sensitive to the triangle diagram but not the box diagram.

The feasibility study of detecting Higgs pair production with future update of LHC (high-luminosity upgrade, HL-LHC, which aims to accumulate a total integrated luminosity of 3 ab^{-1}[4]) has been done for different decay channel, for example, the gluon fusion channel(which is the dominant decay channel), ,$b\bar{b}\gamma\gamma$[5], $b\bar{b}\tau^+\tau^-$[6], $b\bar{b}W^+W^-$[7] $b\bar{b}b\bar{b}$[1], etc. For this study, we are focusing on the $b\bar{b}b\bar{b}$ channel. We are running a Monte Carlo simulation of the Higgs pair production in the gluon-fusion channel with background. The decay products are then reconstructed into jets. We will then simulate the b-jet tagging process in the ATLAS detector. Finally, these tagged b-jets will be utilized in search for Higgs pair production. We aim to research on the impact of applying different tagging algorithms (taggers) on signal significance, $S/\sqrt{B}$ of detecting Higgs pair production.

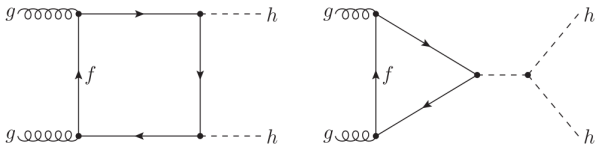

Fig. 1. The box and triangle Feynman diagrams of Higgs pair production in the gluon fusion channel at leading order.

2. CODE SETTING

2.1 Simulations setting

In the study of the Boosting Higgs Pair Production in the $b\bar{b}b\bar{b}$ Final State[1] (we will call the study the "pheno study" from now on), we are running a Monte Carlo simulation of the Higgs pair production using **MadGraph5 aMC@NLO** in the gluon-fusion channel, parton level signal events are then showered with the **Pythia8** Monte Carlo. The background samples are generated at leading order with **SHERPA** v2.1.1.

2.2 Jets reconstruction setting

The jet reconstruction is done by **FastJet** with the anti-k_T algorithm. There are three categories of jets: Small-R jets, Large-R jets, Small-R sub jets. The definition of jets are set to be consistent with the definition of jets in Ref.[2]. The following are the definitions:

—**Large-R jet**:The Large-R jets are defined to be jets with the reconstructed radius $\Delta R \leq 1.0$, transverse momentum $p_T \geq 250$ GeV , pseudo rapidity $|\eta| \leq 2.0$.

—**Small-R jet**:The Small-R jets are defined to be jets with $\Delta R \leq 0.4$, $p_T \geq 40$ GeV, $|\eta| \leq 2.0$.

—**Small-R subjet**:The Small-R subjets are defined to be jets with $\Delta R \leq 0.3$, $p_T \geq 10$ GeV, $|\eta| \leq 2.5$.

The Small-R subjets are ghost-associated to each large-R jets in order to define its subjets. The large-R jets are b-tagged by ghost-

associating anti-k_T R =0.3 (small-R subjets). The probability of tagging a small-R subjet is f_b. The small-R subjet can still be tagged as a b-jet without b-quarks constituent, which is the mistag of b-quarks, the probability of mistagging is given by f_l. In the case of charm quarks presented in the small-R subjet (with no b-quarks), the mistag rate is given by f_c. In the pheno study, the values are set to be: f_b = 0.8, f_l = 0.01, f_c = 0.01.

3. RESULT FROM THE PUB NOTE

3.1 Tagging efficiency and background rejection

In the study of the *Variable Radius, Exclusive-k_T, and Center-of-Mass Subjet Reconstruction for Higgs($\rightarrow b\bar{b}$) Tagging in ATLAS* (we would call this study "pub note" from now on), new subjet tagging techniques (tagger) are investigated, including the use of variable radius trackjets, exclusive-kt subjets, and calorimeter subjets reconstructed in the center-of-mass frame of the Higgs jet (we will call this tagger the "COM tagger" from now on). These three new techniques outperform the fixed radius trackjet tagging technique currently used as the standard method in ATLAS [2] (which is the tagger the pheno study is using), especially in the high p_T region. The performance of these three algorithms are shown in Fig.2. In the figure, the QCD background rejection on the y-axis is defined as followed: 1 over the mistag rate, i.e. 1 over the ratio of background before applying the tagger over the background after applying the tagger (eq.1),

$$QCD\ jet\ rejection = \frac{1}{mistagrate} = \frac{1}{\frac{background\ before\ tagging}{background\ after\ tagging}}. \quad (1)$$

The QCD background rejection indicates the power of rejecting background, bigger the number, stronger the rejecting power of the tagger.

And in Fig.2, the Higgs Jet efficiency on the x-axis is defined as the ratio of the number of Higgs jets after applying the tagger over the number of Higgs jets before applying the tagger (eq. 2),

$$Higgs\ jet\ efficiency = \frac{\#\ of\ Higgs\ Jets\ before\ tagging}{\#\ of\ Higgs\ Jets\ after\ tagging}. \quad (2)$$

The Higgs jet efficiency indicates the power of accepting Higgs jet (signal), bigger the number, stronger the accepting power of the tagger.

The QCD background rejection is given as a function of the double b-tagging Higgs jet efficiency and in different region transverse

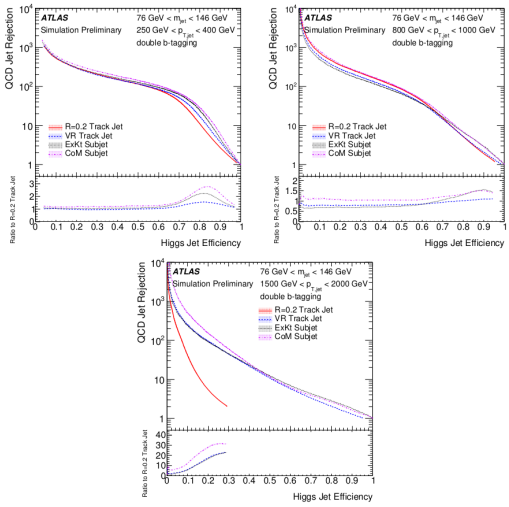

Fig. 2. QCD jet rejection as a function of Higgs jet efficiency at different p_T range.

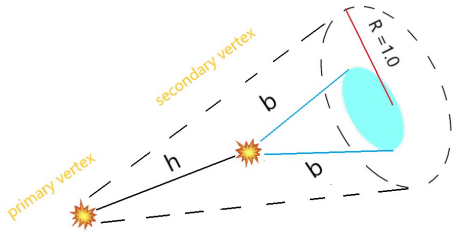

Fig. 3. A tagged Higgs jet.

momentum of the jets for different reconstruction algorithm. We can see that out of the four taggers, the COM tagger perform the best (with combination of large rejection and large efficiency), so in this study we will be applying the result of the COM tagger.

Notice that this tagging efficiency is the efficiency of tagging a large-R jet with a Higgs boson inside (Higgs jet) with 2-b quarks (double b-tagged) (Fig.3). This definition of tagging efficiency is different from the tagging efficiency used in the pheno study since the taggers are different. We have to be careful when implementing this pub note result.

We can see higher tagging efficiency leads to lower background rejection, and this is why we want to find the balance of keeping more events and rejecting more background. This relation changes significantly with different p_T, and this might lead to a smaller signal significance $S/\sqrt{B}$ with constant tagging efficiency, i.e. using a high tagging efficiency can have a good background rejection in low pT region but poor background rejection in the high p_T region.

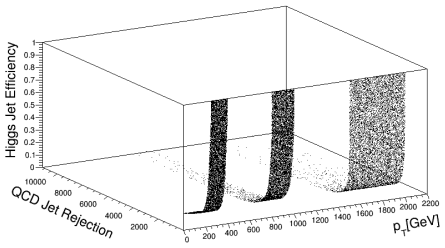

Fig. 4. A 3-D view of the QCD jet rejection as a function of Higgs jet efficiency at different p_T range.

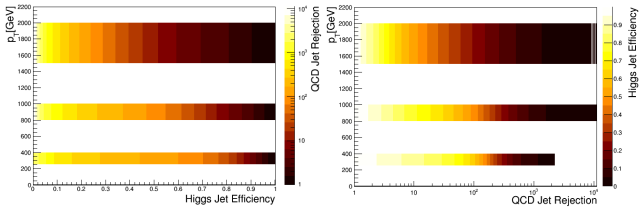

Fig. 5. The projection on the p_T, efficiency axis and on the p_T, rejection axis.

3.2 A 3-D view of the result

To have a clear view of this relation, we can combine the three separate graphs in Fig. 2 to a 3-D graph (Fig. 4), with x-axis the p_T, y-axis the QCD jet rejection, z-axis the Higgs jet efficiency.

The 2-D projections on the axis of p_T and background rejection, p_T and tagging efficiency are shown in Fig. 5.

3.3 Linear extrapolation

It is clear that the relation is discrete in p_T, in the pheno study we account for all large-R jet having $p_T \geq 200$ GeV. To implement this relation we would need to have a function covering the whole region of 2000 GeV $\geq p_T \geq$ 250 GeV. Therefore we would need to extrapolate the relation between the gaps. The following is the binning of the p_T regions: 250-400, 400-600, 600-800, 800-1000, 1000-1250,1250-1500, 1500-2000, in the unit of GeV. The linear extrapolation is done as following: taking the functions of rejection and efficiency at the mid points of the 250-400, 800-1000 and 1500-2000, which is p_T = 325, 900, 1750, and assuming these are the functions for the corresponding p_T regions. We then have three lines at p_T = 325, 900, 1750. We can then connect these three lines, impose the binning (400-600, 600-800, etc.), and then take the function of rejection and efficiency at the mid points of the bins to be the function of the corresponding bin. We then have a linear extrapolation of the 3-D graph (Fig. 6). The 2-D projections on the axis of p_T and background rejection, p_T and tagging efficiency are shown in Fig. 7.

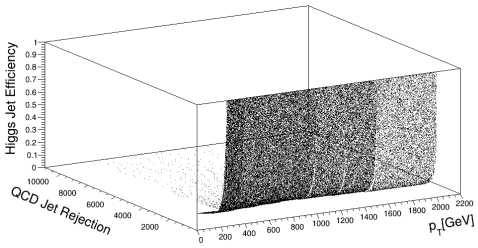

Fig. 6. A 3-D view of the QCD jet rejection as a function of Higgs jet efficiency at different p_T range, with linear extrapolation.

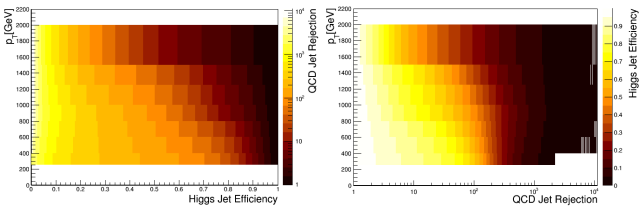

Fig. 7. The projection on the p_T, efficiency axis and on the p_T, rejection axis.

3.4 Fitting the result

To use this relation, we have to fit for a function first. There are two ways to do the extrapolation and fitting, we can either extrapolate the graph linearly, then fit the whole 3-D graph, or we can fit for the function separately for the 3 p_T region and then do the extrapolation. Using the first method might lead to a very complicated function with lots of parameters, so here we can use the second way. In the code we would be using relatively high tagging efficiency, therefore we can keep only the part where efficiency ≥ 0.3. The result of fitting is shown in Fig. 8. The model used for the fitting is an exponential model:

$$ae^{-bx-cx^2-dx^3-ex^4}. \tag{3}$$

The fitting looks good by eyes as the fitted line almost overlap with the data line, to see further whether these fits are good enough, the chi square is calculated for each fitting. The chi square is given as follow:

$$\chi = \sum_i \frac{(O_i - C_i)^2}{O_i}, \tag{4}$$

where O_i is the observation data, and C_i is the calculated data. To avoid infinity, we assume the O_i is approximately C_i in the denominator. The chi square values for the three fitting with the fitted parameters are shown in Table I.

We used 35 data points for fitting, the degree of freedom $\nu = n - m$ is the number of data points n minus the number of fitting parameters m, hence $\nu = 30$ in this case. Chi square of $\nu = 30$ with 0.995 confidence is 13.787. The values of reduced chi square

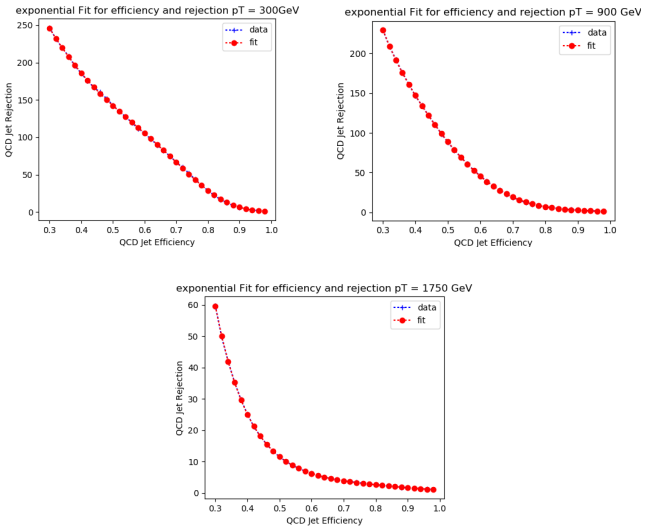

Fig. 8. Fitting exponentially for the background rejection as a function of tagging efficiency in different p_T region.

Table I. Result of fitting with $ae^{-bx-cx^2-dx^3-ex^4}$

p_T region	Chi square	fitted parameters
250-400 GeV	0.5928	254.56 -5.75 33.50 -57.21 35.69
800-1000 GeV	0.2737	5390.35 21.40 -55.90 75.15 -32.19
1500-2000 GeV	0.0407	331.49 -0.86 35.83 -53.71 24.67

are all much smaller than 1, which is an evidence that the fits are good enough. We can then extrapolate between the gaps using these fitted function, and use it to find out the optimal tagging efficiency for each p_T region.

3.5 Optimal value of the tagging efficiency

Generally we can either aim for the maximal signal over background ratio (S/B) or the maximal signal significance ($S/\sqrt{B}$), for this study we choose to maximise the signal significance $S/\sqrt{B}$, but both of them are valid evaluation. To maximise $S/\sqrt{B}$, we want to have high tagging efficiency with high background rejection. With eq. 5, and recall the definition of Higgs Jet efficiency and background in section 3.1, it should be clear that the optimal tagging efficiency is obtained with tagging efficiency with the maximum value of efficiency times the square root of the rejection. The result is shown in Tab II.

$$\begin{aligned} Signal\ after\ COM\ tagger &= signal\ after\ cutflow \\ &\quad \times tagging\ efficiency \\ Background\ after\ COM\ tagger &= background\ after \\ &\quad cutflow \div background \\ &\quad rejection \end{aligned} \tag{5}$$

Table II. Optimal tagging efficiency

p_T region	Optimal tagging efficiency	Background Rejection
250-400 GeV	0.59	109.2
400-600 GeV	0.54	108.1
600-800 GeV	0.48	116.2
800-1000 GeV	0.42	99.2
1000-1250 GeV	0.41	106.0
1250-1500 GeV	0.38	83.7
1500-2000 GeV	0.31	54.6

4. THE CUT-BASED METHOD

4.1 Introduction of the cut-based method

To simulate what happens at the LHC, we will run a Monte Carlo simulation of 10000 colliding proton-antiproton events, at centre of mass 14 TeV and integrated luminosity $3ab^{-1}$. We simulate the process which a Higgs pair decays to 4 b-quarks (signal); and other processes which can produce b-quarks (background). Because we are searching Higgs pair production with b-quarks, these "other processes" would be our background. The settings of the simulations of signal (signal samples) and simulations of background (background samples) are explained in section 5. The decay products are then reconstructed into jets, which are cones of particles produced by the hadronization of a quark or gluon (in this study we will not go through the details of the reconstruction algorithm, although interested reader can look up in Ref. [8]). Obviously we want as much signal as possible and as little background as possible. However how do we tell which Monte Carlo events are signal and which are background? To differentiate the background and signal, a traditional cut-based method is used.

The principal of the cut-based method is that while applying a cut (for example, cutting away events with transverse momentum $p_T \leq 100GeV$) we cut away both background and signal; if a cut can cut away much more background than signal, then we are left with a large number of signal, and little background, and then this is possibly a good cut. Hence a sequence of cuts (cutflow) is applied to the Monte Carlo events.

4.2 Setting of the cutflow

The setting of cutflow is based on the pheno study. The parameters of the cuts are the following (some of the parameters are modified to match the pub note's setting):

—**C1a**: Requiring all large-R jets having $p_T \geq 250$ GeV and small-R jets having $p_T \geq 40$ GeV, pseudo rapidity $\eta \geq 2.5$. Each event is required to have at least two large-R jets in it.

—**C1b**: The two leading large-R jets must be mass-drop tagged.

—**C1c**: The invariant mass of the two Higgs candidates are required to lie within the mass window of $76 \leq m_H \leq 146$ GeV.

Table III. Cutflow of the Monte Carlo events, check at detector level

Cut	Number of Monte Carlo events
Starting	100000
C1a	15883
C1b	12139
C1c	6059
C2	6059
C3	3403
C4	1091

—**C2**: Apply the b-tagger.

In the pheno study, there are 3 categories of event, we will only be considering the boosted category, i.e.the event which there are at least two large-R jets (strictly speaking these two large-R jets are b-tagged as well, but we will turn off the tagger later on. We will keep the requirement of having at least two for simplicity, as the other two categories are more complicated). Recall from last section, the Higgs jet tagging efficiency is defined as tagging a large-R jet to be double b-tagged with a Higgs inside, i.e. having two b-quarks and one Higgs within the large-R jet. Before implementing this result, we want to check whether there are enough events with a Higgs and 2 b-quarks in the large-R jet (Fig.3). This study can not proceed if there are very few events satisfy this requirement. Here we add two more cuts here to check:

—**C3**:Requiring both large-R jets to have one Higgs inside.

—**C4**: Requiring both large-R jets to be double b-tagged.

The **C3** cut is done as follows: from the signal samples, we find the true "final state" (it's not the stable final state, but the final state before decaying) Higgs Bosons and put their 4-momentum vectors in a container. We then determine the ΔR of these Higgs Bosons with respect to the reconstructed Large-R jets. If $\Delta R \leq 1.0$, we can say these Higgs Bosons are within the Large-R jets. The **C4** cut is done as follows: Using the b-tagger in the pheno code, we can determine the number of tagged b-jets inside the Large-R jets. We can then require the number of b-jets inside the Large-R jet to be 2.

4.3 Sanity Check at detector level

Here we have followed the full procedure of reconstructing jets and simulating the detector. We then use the result of the detector simulations to require the large-R jets to satisfy the definition of Higgs jet (Fig. 3), and this is exactly what the cut **C4** is doing. Since we have done the simulations of dectector, this is a check of the dectector level. The result is shown in Tab III.

We can see C3 and C4 cuts cut away about $2/3$ of the events.

Table IV. Cutflow of the Monte Carlo events, check at events level

Cut	Number of Monte Carlo events
Starting	100000
C1a	15883
C1b	12139
C1c	6059
C3	3403
C4′	544

4.4 Sanity check at event level

The previous check is done with the result of simulations of the detector, it would be helpful to do a check without the tagger, i.e. we can directly look at the simulations of the collisions (event level) and find out the number of Monte Carlo events which satisfy the definition of the Higgs jet (Fig.3). Therefore we will turn off the tagger (**C2**) and apply a new cut **C4′**.

—**C4′**: Requiring both large-R jets to have two true b-quarks.

The **C4′** is similar to the **C4** cut. From the signal samples, we find the true "final state" b-quarks and put their 4-momentum vectors in a container. We then determine the ΔR of these b-quarks with respect to the reconstructed Large-R jets. If $\Delta R \leq 1.0$, we can say these b-quarks are within the Large-R jets. We allow any combination of b-quarks in the Large-R jet, i.e. we allow having 2 b-quarks or 2 $\bar{b}$-quarks in one Large-R jet, not restricting to only $b\bar{b}$ pair.

The cut flow is now **C1a**, **C1b**, **C1c**, **C3**, **C4′**, agian notice that **C2** (the tagger) is not used here. The result of the cutflow is shown in Tab IV. We can see that there is still a decent amount of events left over. We can hence conclude that we have enough number of events for analysis at detector and event level.

5. IMPLEMENTATION OF THE PUB NOTE RESULT

5.1 Simulations of the COM tagger

Now that we have the optimal tagging efficiency and enough events, we can implement the result into the pheno code. This is achieved by calculating the signal and background cross sections using the pheno code, in different regions of p_T with the optimal tagging efficiency and the corresponding background rejection. Since we are looking at the impact of applying the more advanced COM tagger, we will be turning off the tagger used in the pheno code, i.e. we will be running the simulations with **C1a**, **C1b**, **C1c** but no **C2**. After these cuts applied, we can then simulate the COM tagger with eq. 5.

We will then have the signal and background in different p_T regions accordingly. Since we are simulating the HL-LHC, the lumi-

Table V. Result of background samples' cross sections, with various background rejection

Background samples:	**2b2j** $[fb]$	**4b** $[fb]$	**4j** $[fb]$	**total background** $[fb]$	**total background after tagging**$[fb]$
250-400 GeV	$16.77 \cdot 10^3$	$13.32 \cdot 10^3$	$22.26 \cdot 10^3$	$52.35 \cdot 10^3$	479.4
400-600 GeV	$8.73 \cdot 10^3$	$5.16 \cdot 10^3$	$10.02 \cdot 10^3$	$23.91 \cdot 10^3$	92.7
600-800 GeV	1530	1770	2730	6030	23.49
800-1000 GeV	390	330	75	795	8.01
1000-1250 GeV	390	300	270	960	9.06
1250-1500 GeV	30	90	150	270	3.24
1500-2000 GeV	90	60	30	180	3.30

Table VI. Result of Signal samples' cross section, with various tagging efficiency

	total signal $[fb]$	**total signal after tagging**$[fb]$
250-400 GeV	0.4244	0.2504
400-600 GeV	0.09240	0.04993
600-800 GeV	$7.529{\cdot}10^{-3}$	$3.614{\cdot}10^{-3}$
800-1000 GeV	$8.500{\cdot}10^{-4}$	$3.570{\cdot}10^{-4}$
1000-1250 GeV	$2.841{\cdot}10^{-4}$	$1.165{\cdot}10^{-4}$
1250-1500 GeV	$14.21{\cdot}10^{-5}$	$5.398 \cdot 10^{-5}$
1500-2000 GeV	$32.07 \cdot 10^{-4}$	$9.940 \cdot 10^{-4}$

nosity is $3ab^{-1} = 3000fb^{-1}$ by assumption, and the rate of reaction is defined as follows (eq. 6):

$$Rate\ of\ reaction = cross\ section\ \times luminosity \tag{6}$$

In the pheno code the cross section is conveniently calculated along with the Monte Carlo events. Then we can calculate signal and background after the tagger in terms of reaction rate, with cross sections given by the code. We can then sum over the cross sections over all p_T region and multiply the luminosity, which gives the reaction rate of the signal, and then divided by the square root of the reaction rate of the background, i.e.

$$S/\sqrt{B} = \frac{\sum_i S_i \cdot L}{\sqrt{\sum_i B_i \cdot L}} = \frac{\sum_i S_i}{\sqrt{\sum_i B_i}} \cdot \sqrt{L}, \tag{7}$$

where i is the region of p_T, and S_i is the signal cross section after the COM tagger applied in p_T region i, and similarly B_i is the background cross section with the COM tagger applied in p_T region i, and L is the luminosity.

5.2 Background sample result

The background samples are generated at leading order with **SHERPA** v2.1.1. We account for relevant background processes that can mimic the hh $\rightarrow$ 4b signal process. This includes QCD 4b multi-jet production, as well as QCD 2b2j and 4j production, the top quark pair production is assumed to have small contribution so we can ignore for this study. We divide each background sample into 30 separated jobs, each job will give a result of cross section of background after the cutflow applied. We then combine these 30 cross-section values to give the total cross section of each sample. We can then simulate the COM tagger with eq. 5.

The background is then given in terms of reaction rate, i.e. the cross section of background $\times$ the luminosity (recall that the luminosity for HL-LHC is 3 ab^{-1} = 3000 fb^{-1}). The result of the cross sections of the background samples in different p_T region is shown in Tab V.

5.3 Signal sample result

The Higgs pair production is simulated at leading order (LO). The model for gluon-fusion includes mass effects from the exact form factors for the top-quark triangle and box loops (Fig1). We also assume there is no pile-up in the detector. Similarly we separate the signal sample into 10 jobs, each job will give the result of cross section after the cutflow, and we combine these 10 jobs to obtain the total cross section of the signal. Then we can simulate the COM tagger with eq. 5. The result of signal in each p_T region is shown in Tab VI.

5.4 Result of $S/\sqrt{B}$

With equation 6 and equation 7, we can now calculate the $S/\sqrt{B}$ ratio. The $S/\sqrt{B}$ ratio in the pheno paper, with the standard tagger using in ATLAS is 0.5. The $S/\sqrt{B}$ ratio with optimal tagging efficiency is 0.67, we can see there is an clear increase of the $S/\sqrt{B}$. Although the COM tagger outperforms significantly the tagger used in the pheno paper in the high p_T region (Fig. 2), the cross section of the signal drops off very quickly with p_T increases. Therefore the dominant contribution of the signal significance comes from the low p_T region, which we can see in Fig. 2 the COM tagger slightly outperforms the tagger used in the pheno study. This also justifies the improved result of the signal significance.

6. CONCLUSION

As shown in a study of the performance of b-jet identification in the ATLAS detector [9] in Fig. 9, in the real ATLAS detector, the

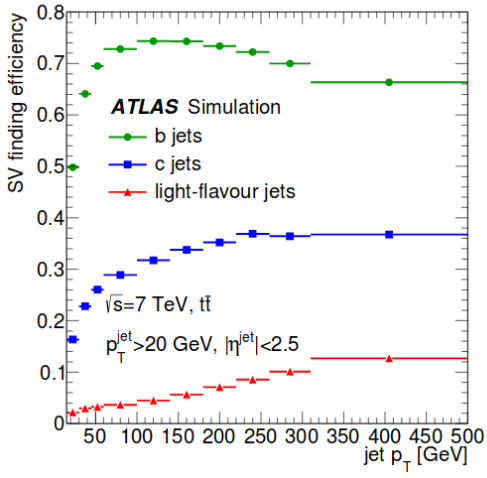

Fig. 9. Performance of the b jets identification[9]

tagging efficiency would vary for jet with different p_T. Therefore simulation of detector using a various tagging efficiency with p_T dependency would be more realistic. On the same time, using the more advanced COM tagger increases the signal significance from 0.5 to 0.67, with p_T depending tagging efficiency (optimal tagging efficiency is obtained in section 3.5).

This study also gives an estimation of maximal signal significance which can be obtained with the COM tagger with traditional cut-based method. Although in the real detector, the tagging efficiency would not behave the same as the optimal tagging efficiency as p_T varies; considering for the COM tagger, the product of tagging efficiency and the square root of the background rejection (this product is used to find the optimal tagging efficiency in section 3.5, and it's proportional to the signal significance) is varying relatively slowly with tagging efficiency varying (at $p_T = 300$ GeV, efficiency = 0.3: $efficiency \cdot \sqrt{rejection} \approx$ 4.7, efficiency = 0.5: $efficiency \cdot \sqrt{rejection} \approx 6.1$, efficiency = 0.7: $efficiency \cdot \sqrt{rejection} \approx 6.0$) and the dominant contribution of the signal significance comes from the lower p_T region as shown in Tab. VIin section 5.1, we can safely say that in the real ATLAS detector the signal significance would not deviate far from 0.67.

In order to push the $S/\sqrt{B}$ further to the observation level, we could apply different analysis method, such as the multivariate analysis which is based on artificial network (It is shown in the pheno study that applying the multivariate analysis, we can further improve the signal significance from 0.5 to 2.7). A combination of the MVA method with a more advanced tagger has the possibility to even increase the signal significance further.

7. ACKNOWLEDGEMENT

The success and final outcome of this project required a lot of guidance and assistance from many people and I am extremely privileged to have got this all along the completion of my project. I would like to express my special thanks of gratitude to my supervisor Professor Cigdem Issever for providing me an opportunity to do the project work in Higgs boson study and giving me all support and guidance which made me complete the project. I owe my deep gratitude to Lydia Beresford and Nurfikri Bin Norjoharuddeen who took keen interest on my project and guide me all along with great passion. I heartily thank the 2H4b pheno group for all the valuable advice and guidance.

REFERENCES

1.Behr, J.K., Bortoletto, D., Frost, J.A. et al., *Boosting Higgs Pair Production in the $b\bar{b}b\bar{b}$ Final State with Multivariate Techniques, Eur. Phys. J.* **C76** (2016) 386. DOI: https://doi.org/10.1140/epjc/s10052-016-4215-5.

2.**ATLAS** collaboration, *Variable Radius, Exclusive-k_T, and Center-of-Mass Subjet Reconstruction for Higgs($\rightarrow b\bar{b}$) Tagging in ATLAS, ATL-PHYS-PUB-2017-010* (2017) DOI: https://cds.cern.ch/record/2268678?ln=en

3.J. Baglio, A. Djouadi, R. Grober, M. Muhlleitner, J. Quevillon, et al., *The measurement of the Higgs self-coupling at the LHC: theoretical status, JHEP* **1304** (2013) 151, arXiv:1212.5581.

4.**ATLAS** Collaboration, *Physics at a High-Luminosity LHC with ATLAS*, arXiv: 1307.7292.

5.U. Baur, T. Plehn, and D. L. Rainwater, *Probing the Higgs selfcoupling at hadron colliders using rare decays, Phys.Rev.* **D69** (2004) 053004, hep-ph/0310056.

6.U. Baur, T. Plehn, and D. L. Rainwater, *Examining the Higgs boson potential at lepton and hadron colliders: A Comparative analysis, Phys.Rev.* **D68** (2003) 033001, hep-ph/0304015.

7.Andreas Papaefstathiou, Li Lin Yang, and José Zurita, *Higgs boson pair production at the LHC in the $b\bar{b}W^+W^-$ channel,Phys. Rev.* **D87**, (2013)011301(R), DOI:10.1103/PhysRevD.87.011301.

8.Matteo Cacciari, Gavin P. Salam, Gregory Soyez, *The anti-$k_t$jetclusteringalgorithm*, $arXiv : 0802.1189$.

9.**ATLAS** collaboration, *Performance of b-Jet Identification in the ATLAS Experiment*, arXiv:1512.01094.